

Magnetic properties of pure and Gd doped EuO probed by NMR

Arnaud Comment* and Jean-Philippe Ansermet

*Department of Physics and Materials Research Laboratory,
University of Illinois at Urbana-Champaign, 1110 West Green Street, Urbana, Illinois 61801-3080
and Institut de Physique des Nanostructures, Ecole Polytechnique
Fédérale de Lausanne, CH-1015 Lausanne-EPFL, Switzerland*

Charles P. Slichter

*Department of Physics and Materials Research Laboratory,
University of Illinois at Urbana-Champaign, 1110 West Green Street, Urbana, Illinois 61801-3080*

Heesuk Rho,[†] Clark S. Snow, and S. Lance Cooper

*Materials Research Laboratory, University of Illinois at Urbana-Champaign,
104 South Goodwin Ave, Urbana, Illinois 61801-3080*

(Dated: November 8, 2018)

An Eu NMR study in the ferromagnetic phase of pure and Gd doped EuO was performed. A complete description of the NMR lineshape of pure EuO allowed for the influence of doping EuO with Gd impurities to be highlighted. The presence of a temperature dependent static magnetic inhomogeneity in Gd doped EuO was demonstrated by studying the temperature dependence of the lineshapes. The results suggest that the inhomogeneity in 0.6% Gd doped EuO is linked to colossal magnetoresistance. The measurement of the spin-lattice relaxation times as a function of temperature led to the determination of the value of the exchange integral J as a function of Gd doping. It was found that J is temperature independent and spatially homogeneous for all the samples and that its value increases abruptly with increasing Gd doping.

PACS numbers: 71.30.+h, 75.30.m, 76.60.k, 75.50.Pp

I. INTRODUCTION

Numerous studies on EuO have been published since the discovery of the ferromagnetic phase of this compound by Matthias *et al.* in 1970,¹ and still very recently several experimental research projects have been conducted on pure and Gd doped EuO.^{2,3,4,5} There are several reasons for this interest: first, EuO is one of the few natural ferromagnetic semiconductors. Second, there is currently a great deal of attention on ferromagnetic semiconductors like (Ga,Mn)As and (In,Mn)As.⁶ Third, a new field called spintronics has been developed around the possibilities of using the spin degree of freedom of the electron in solid-state electronics.⁷ Fourth, EuO is an ideal system for testing new theories in magnetism, in particular the recent developments made on the Kondo-lattice model. The localized magnetic moments of the half-filled $4f$ -shell of the Eu atoms and the existence of a conduction band makes EuO an appropriate system to test the Kondo-lattice model.^{8,9,10} In addition, the low magnetic anisotropy of the material along with the localized $J = S = 7/2$ spins of the Eu^{2+} ions makes europium monoxide a nearly ideal Heisenberg ferromagnet.

Another peculiarity of EuO compounds such as O-rich EuO and Gd doped EuO is their colossal magnetoresistance (CMR).^{11,12,13,14,15} CMR has also been observed in manganites. Nuclear magnetic resonance (NMR) has been proven to be a good technique to study local magnetic microstructures such as stripes and magnetic polarons.^{16,17} However, to our knowledge, such a

study in europium chalcogenides has never been performed and NMR data in EuO have been published only for temperatures far below the transition temperature, i.e. far below the temperatures at which CMR effect is observed in electron doped EuO. The main reason that led us to study europium chalcogenides rather than manganites is that the former are simple diatomic cubic crystals whereas the structure of the latter is substantially more complex. Consequently, studies of the (Eu,Gd)O system should allow us to extract detailed information from NMR measurements without the complications of numerous exotic phenomena of manganites such as phase separation, charge and orbital ordering, and Jahn-Teller distortions.

In this paper we present NMR results on single crystals of pure and Gd doped EuO. In Gd doped EuO, Gd atoms play the role of electron donors and are expected to affect the localized magnetism of EuO negligibly. One goal of this study was to examine the effect of Gd doping on the magnetic properties of EuO. In Section II, we describe the characteristics of the samples we studied and give a detailed analysis of the NMR lineshape of Eu in EuO. In Section III, we describe the temperature dependence of the relaxation times of the Eu nuclear spins. Finally, in Section IV, we discuss the properties of the lineshape of Eu in Gd doped EuO and discuss some models to link our observations to CMR behavior.

II. SAMPLE CHARACTERIZATION

We studied four types of samples: pure EuO, 0.6%, 2%, and 4.3% Gd doped EuO. According to Samokhvalov *et al.*, these samples can be categorized as follows:¹⁴ samples of pure and stoichiometric EuO are insulators; samples with a Gd concentration smaller than about 1.5% undergo a metal-insulator transition (MIT) when the temperature is increased above about 30 K, the low temperature regime being metallic; samples containing a Gd concentration larger than about 1.5% have a metallic behavior at all temperatures. Godart *et al.* also observe similar behavior in Gd doped EuO,¹⁵ but not Schoenes and Wachter.¹⁸

A. Spectrometer

The spin-spin relaxation time T_2 of ^{151}Eu and ^{153}Eu nuclei in pure and Gd doped EuO can be very short, especially when the temperature is increased towards the transition temperature. To measure signals with short T_2 , we built a spectrometer with the following specifics: minimum pulse length of 20 ns, minimum delay between two pulses of 300 ns, recovery time of the receiver of 300 ns, and maximum sampling rate of the receiver of 1GSample/s. The high sampling rate is needed because of the short echoes.¹⁹

In order to detect the signal using a short delay between the two excitation pulses of a spin-echo sequence, it was necessary to use a low Q tank circuit. Typically, we used a Q of about 10, which corresponds to a recovery time of about 300 ns. Note that the use of such a small value of Q is possible because of the presence of an amplification factor, a property inherent to magnetic materials.

B. Remarks on amplification factor

In ferromagnetic materials, the excitation RF field \mathbf{H}_1 acting on the nuclear spins is amplified by a factor η via the magnetic susceptibility of the unpaired electron spins.²⁰ In EuO the magnetic anisotropy is low and consequently the amplification factor for nuclei in domain walls is not substantially stronger than for nuclei in domains. Indeed, the amplification in domains is given by $\eta_{Domain} = |\mathbf{H}_{hf}|/|\mathbf{H}_{an} + \mathbf{H}_{int}|$, where \mathbf{H}_{hf} is the hyperfine field, \mathbf{H}_{an} is the anisotropy field and \mathbf{H}_{int} is the internal field defined as the sum of the external field, the demagnetization field and the Lorentz field²¹. The amplification in a domain wall of a spherical particle is given by $\eta_{DW} = \pi D |\mathbf{H}_{hf}| / (N \delta |\mathbf{M}(T)|)$, where N is the demagnetization factor of the domain, D is the domain size, δ is the width of the domain wall and $\mathbf{M}(T)$ is the magnetization in domains at temperature T,²² and there-

fore:

$$\frac{\eta_{Domain}}{\eta_{DW}} = \frac{N}{\pi} \frac{\delta}{D} \frac{|\mathbf{M}(T)|}{|\mathbf{H}_{an}|}. \quad (1)$$

From the study of the dynamic susceptibility on an EuO sphere, Flosdorff *et al.* have determined that $\delta/D \cong 0.08 |\mathbf{M}(T=0)|/|\mathbf{M}(T)|$.²³ Then, by taking $N = 4\pi/3$, assuming a spherical domain, $|\mathbf{M}(T = 4.2 \text{ K})| = 1623 \text{ emu/cm}^3$,²⁴ and $|\mathbf{H}_{an}(T = 4.2 \text{ K})| = 247.5 \pm 2.5 \text{ Oe}$,²⁵ we obtain $\eta_{Domain}/\eta_{DW} \cong 0.7$. Therefore, at 4.2 K the amplification in domains is only slightly weaker than the amplification in domain walls. Moreover, since $|\mathbf{H}_{an}(T)| \propto (|\mathbf{M}(T)|/|\mathbf{M}(T=0)|)^5$,²⁶ the ratio (1) increases rather rapidly with increasing temperature. It appears then that we cannot a priori decide if the NMR signal will be dominated by nuclei in domains or nuclei in domain walls. However, several considerations indicate that what we observe does not depend on whether the nuclei are located in walls or in domain walls. First, the lineshape we observed is similar to the one observed in previous experiments done in field high enough to suppress domain walls.^{27,28,29} Second, in a field of 4 T, when all domain walls are suppressed, we observed the same temperature dependence of the relaxation times as in zero-field. Therefore, in zero-field we did not observe any additional relaxation mechanism related to the presence of domain walls such as a relaxation mechanism due to domain walls motion.

C. Magnetization vs. temperature

In ferromagnetic materials, the hyperfine field is proportional to the magnetization. Therefore, if we assume that the nuclear dipolar field is negligible compared to the hyperfine field, a measurement of the temperature dependence of the zero-field ^{153}Eu NMR frequency gives the temperature dependence of the magnetization. The frequency measurements are presented in Fig. 1. We determined the Curie temperature by measuring the susceptibility χ in the paramagnetic regime, plotting $1/\chi$ as a function of temperature and determining the temperature at which the extrapolated $1/\chi$ line reaches zero. This temperature corresponds to the so-called paramagnetic Curie temperature θ_C . It is important to note that, according to the results of Samokhvalov,³⁰ in Gd doped EuO samples the value of θ_C is larger than the value of the Curie temperature T_C , the temperature above which the spontaneous magnetization vanishes. In particular, the value of T_C of both pure and 0.6% Gd doped EuO is about 69.55 K.

Although the magnetization in these systems is not well described by mean-field theory since spin waves play a crucial role at low temperatures, we plotted Brillouin curves along with the data as rough approximations of the entire magnetization curves intended to serve as

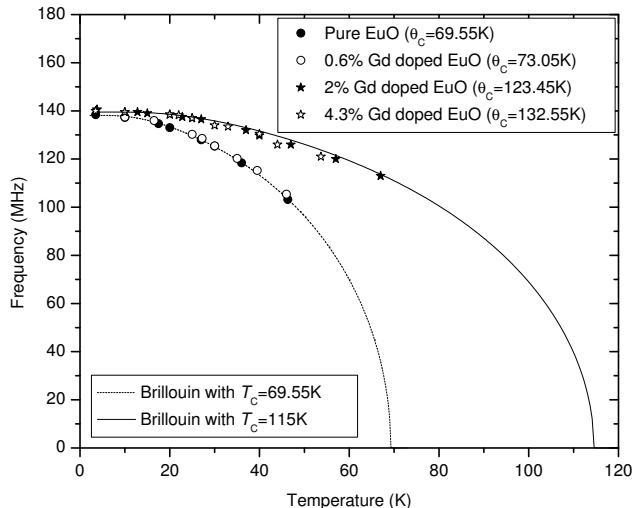


FIG. 1: Zero-field NMR frequency of the center of the NMR line of pure and Gd doped EuO vs. temperature. Brillouin functions are plotted along with the data.

guides for the eyes. The data shown in Fig. 1 are comparable to the data published by Mauger *et al.*³¹ This is one of the indications that our samples are consistent with those of other authors, though coming from different sources at different times. Other such signs of consistency among samples will come from NMR data, as shown below.

Kapusta *et al.* measured the temperature dependence of the frequency in various manganites and observed that the hyperfine field did not vanish at $T = T_C$.³² The authors concluded that there was a residual magnetization above T_C that could be due to the presence of ferromagnetic regions such as magnetic polarons. We could not observe the resonance near T_C , but our data differ qualitatively since these authors observe nearly no drop in magnetization up to T_C whereas we observed that the resonance frequencies already decrease substantially if T is increased up to $\frac{1}{2}T_C$.

D. Lineshape in pure EuO at 4.2 K

The NMR lineshape of ^{153}Eu in single crystals of pure EuO at 4.2 K has already been studied several times. In 1966, Boyd found a single sharp resonance using continuous wave NMR.³³ Later, Raj *et al.* observed that the zero-field lineshape is composed of a sharp central line and two wings but they did not discuss the broadening mechanisms.³⁴ Then, Fekete *et al.* observed five quadrupolar lines in a saturation field of 2 T.²⁷ Finally, Arons *et al.* observed a zero-field lineshape that they described as a sharp line on top of a broad line.^{28,29,35} They claimed that the sharp line corresponded to the signal from nuclei located in domain walls and that the broad line corresponded to the signal from nuclei in domains.

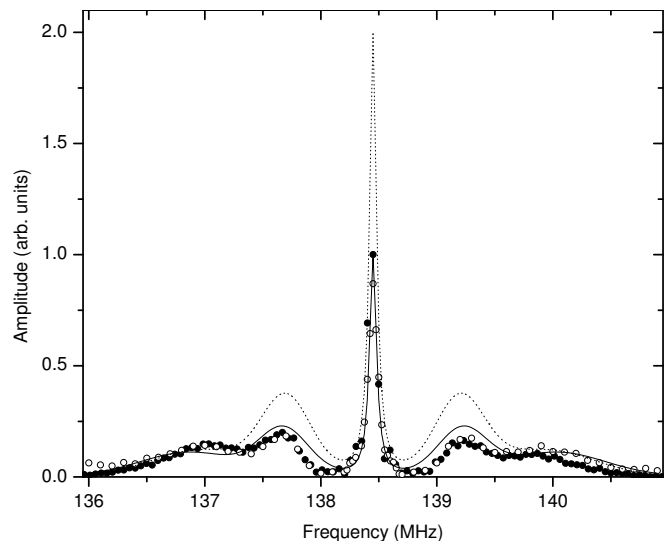


FIG. 2: Zero-field lineshape of ^{153}Eu in EuO at 4.2 K: the black dots correspond to the FT of the echo and the open circles to the point-by-point measurement. The dotted line is the fit of the data using (3) and the plain line is the same fit corrected for T_2 effects.

We present in Fig. 2 the zero-field lineshape of ^{153}Eu in pure EuO that we measured at 4.2 K. We determined the lineshape by two different techniques: on one hand, we measured the echo integral at a certain number of discrete values of frequency (point-by-point measurement). Alternatively, we performed a Fourier transform (FT) of the echo measured at the frequency of the central line. As shown in Fig. 2, both methods give an almost identical lineshape.

Since contradictory results and analysis of the lineshape of ^{153}Eu in pure EuO at 4.2 K were published, we present here our own analysis. Because the Eu sites in EuO have a nominal cubic symmetry, we expected to observe a single narrow line. However, as shown in Fig. 2, we observed an intense central peak and two wings with a structure suggesting that each wing is composed of two broadened lines. In order to distinguish between the broadening due to electric field gradients (EFGs) and the broadening due to the magnetic environment of the nuclei, we took advantage of the fact that there are two isotopes of europium with similar natural abundance. The gyromagnetic ratio and the electric quadrupole moment of the two isotopes are shown in Table I. The zero-field lineshape of ^{151}Eu in pure EuO at 4.2 K is shown in Fig. 3. By comparing the ^{153}Eu and the ^{151}Eu line at 4.2 K we observed that the lines cannot be described solely by magnetic broadening or by quadrupole electrical broadening. We therefore came to the conclusion that the broadening was due to a combination of both effects. We will discuss the origin of such a broadening in Sect. IV A.

In the presence of EFGs, since ^{153}Eu has a spin $I = 5/2$, we expected to observe five lines all separated by the same frequency interval $\Delta\nu_Q$ and with intensity ratios

TABLE I: Spin, natural abundance, gyromagnetic ratio, and electric quadrupole moment of the two europium isotopes.³⁶

	Spin	Nat. abund. (%)	$\gamma_n/2\pi$ (MHz/T)	Q (barn)
¹⁵³ Eu	5/2	52.19	4.6745	2.41
¹⁵¹ Eu	5/2	47.81	10.5856	0.903

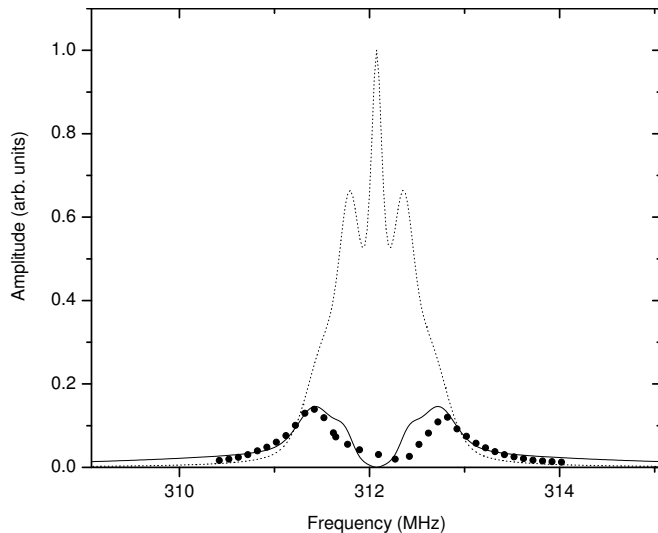


FIG. 3: Zero-field lineshape of ¹⁵¹Eu in EuO at 4.2 K: the black dots correspond to the point-by-point measurement. The dotted line is the computed lineshape and the plain line is the same computed lineshape corrected for T_2 effects.

$$f(\nu) = \sum_{m=-2}^{m=2} \left(1 - \frac{m^2}{9}\right) \frac{\frac{1}{2}\Gamma}{\pi^{3/2}} \int_{-\infty}^{\infty} \frac{e^{-t^2}}{(\nu - (\nu_0 - m\Delta\nu_Q) - \sqrt{2}|m|\delta_{\Delta\nu_Q}t)^2 + (\frac{1}{2}\Gamma)^2} dt, \quad (3)$$

where Γ represents the FWHM of the magnetic distribution and the factor $(1 - m^2/9)$ accounts for the difference in intensity of the five quadrupolar lines. By fitting the measured ¹⁵³Eu lineshape with this function, it was possible to determine the parameters Γ , $\Delta\nu_Q$ and $\delta_{\Delta\nu_Q}$. The fit is represented by a dotted line in Fig. 2 and the deduced values of the fitting parameters are shown in Table II. However, there was another characteristic that needed to be taken into account: Raj *et al.* showed that the ¹⁵³Eu spin-spin relaxation time in pure EuO is short and frequency dependent and, as a consequence, some of the nuclei might not be observed if the delay between the excitation pulses is too long.³⁴ They observed that the intensity of the central part of the line is strongly reduced. We demonstrated this phenomena in Fig. 4 where we plotted the FT of the echo measured with two different delays.⁶³ We took this effect into account in the computation of the lineshape of ¹⁵³Eu by multiplying (3) by an approximated shape of the frequency distribution of T_2

5:8:9:8:5.³⁷ We tried to reproduce the observed lineshape theoretically by assuming a distribution in EFGs and a magnetic broadening. We described the inhomogeneities in the EFGs with a Gaussian distribution leading to a distribution in frequency $G(\nu)$ of second moment $\delta_{\Delta\nu_Q}$ that broadens the five lines. As will be discussed in Section III B, a Lorentzian distribution describes correctly the magnetic broadening. The broadening resulting from these two mechanisms is a convolution of the two distribution functions. The convolution of a Gaussian and a Lorentzian gives a Voigt function, i.e., a function of the form

$$V(\nu) = \frac{\frac{1}{2}\Gamma}{\pi^{3/2}} \int_{-\infty}^{\infty} \frac{e^{-t^2}}{(\nu - \nu_0 - \sqrt{2}\sigma t)^2 + (\frac{1}{2}\Gamma)^2} dt, \quad (2)$$

where Γ is the full width at half maximum (FWHM) of the Lorentzian and σ is the second moment of the Gaussian.³⁸ The resulting lineshape is then given by

TABLE II: Values of the lineshape fitting parameters for ¹⁵³Eu along with the deduced parameters for ¹⁵¹Eu.

	Γ [MHz]	$\Delta\nu_Q$ [MHz]	$\delta_{\Delta\nu_Q}$ [MHz]
¹⁵³ Eu	0.072	0.75	0.2
¹⁵¹ Eu	0.163	0.281	0.075

at 4.2 K deduced from our measurements. We will discuss the physical reason for this T_2 distribution in Sect. III B. The computed lineshape is shown in plain line in Fig. 2 along with the measured lineshape.

To verify if our description of the ¹⁵³Eu lineshape was correct, we computed the ¹⁵¹Eu lineshape from the fitting parameters that we determined for ¹⁵³Eu and compared the resulting curve with the measured ¹⁵¹Eu lineshape. We first calculated the parameters for ¹⁵¹Eu using the relations

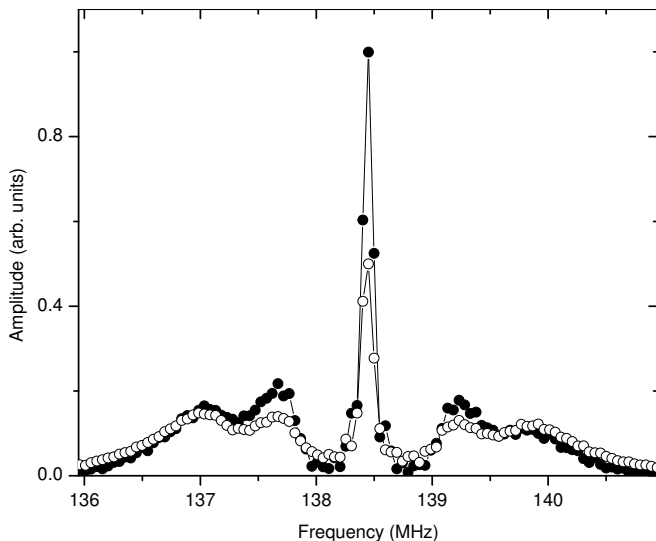


FIG. 4: Zero-field lineshape of ^{153}Eu in EuO at 4.2 K obtained by FT. The black dots correspond to a delay of $10.5 \mu\text{s}$ and the open circles to a delay of $15.5 \mu\text{s}$. This shows the presence of frequency dependent T_2 's (the T_2 's are shorter near the line center).

$$\Gamma_{151} = \frac{151\gamma_n}{153\gamma_n} \Gamma_{153}, \quad (4)$$

$$\Delta\nu_{Q,151} = \frac{151Q}{153Q} \Delta\nu_{Q,153}, \quad (5)$$

$$\delta\Delta\nu_{Q,151} = \frac{151Q}{153Q} \delta\Delta\nu_{Q,153}, \quad (6)$$

where the indices 151 and 153 refer to ^{151}Eu and ^{153}Eu respectively. The computed lineshape is shown as a dotted line in Fig. 3. Then, we deduced the T_2 distribution of ^{151}Eu from the T_2 distribution of ^{153}Eu using the following process: first, since we observed that T_2 at 4.2 K was inversely proportional to γ_n^2 (c.f. Section III B), we divided the amplitude of the distribution by $(^{151}\gamma_n/^{153}\gamma_n)^2$. Second, since T_2 depends on γ_n (and is therefore of magnetic origin), we expected the T_2 distribution to scale with the magnetic distribution. We thus calculated the ^{151}Eu T_2 distribution by multiplying the width of the ^{153}Eu T_2 distribution by $^{151}\gamma_n/^{153}\gamma_n$. The deduced distribution is in good agreement with our data. In order to take into account the fact that the T_2 of the central peak was too short to be detected, we introduced a cutoff in the computed distribution curve. Finally, the T_2 corrected ^{151}Eu lineshape was obtained by multiplying the computed lineshape by the resulting T_2 distribution. The result is plotted in solid line in Fig. 3 along with the measured data. The calculated line was in reasonable agreement with the data, thus confirming our description of the lineshape in terms of a magnetic and a quadrupolar broadening.⁶⁴

The origin of the quadrupolar splitting is most likely

intrinsic to EuO and not due to oxygen vacancies as suggested by Arons *et al.*³⁹ Oxygen vacancies will lead to a clear breaking of the cubic symmetry and therefore, since the quadrupolar moment of Eu is large, the quadrupolar splitting is expected to be large and the Eu sites located next to the vacancies will not contribute to the observed line. Note that the electric quadrupole splitting we observed in zero-field is similar to the one observed by Fekete *et al.* in an external field \mathbf{H}_0 along the easy axis [111] saturating the magnetization ($2 \text{ T} < |\mathbf{H}_0| < 3 \text{ T}$).²⁷

III. EFFECTS OF MAGNONS AND DOPING

The measurement of NMR relaxation times in europium chalcogenides gives some valuable information about the dynamics of their electron spins through the hyperfine coupling. Boyd was the first to report NMR data on EuS,⁴⁰ and together with Charap, used spin-wave theory to deduce values of J_1 and J_2 , respectively the nearest neighbor and next nearest neighbor exchange constant, from the temperature behavior of the NMR frequency of both ^{151}Eu and ^{153}Eu .⁴¹ The first values of NMR relaxation times in EuO were published in 1965 by Uriano and Streever.⁴² Following this work, several groups studied NMR relaxation times and compared their data to spin-wave theory and to the Suhl-Nakamura theory in order to explain their results and to obtain information on the magnetic properties of the system. All the results published concern measurements performed at $T \leq 20.3 \text{ K}$. We extended the study of relaxation times to much higher temperatures and to Gd doped EuO. We determined the influence of doping on the dynamic properties of the electronic magnetization by comparing the relaxation times in EuO to the relaxation times in Gd doped EuO.

A. Spin-lattice relaxation times

We used a saturation recovery sequence to perform T_1 measurements. The sequence destroys the nuclear magnetization by applying a series of pulses before measuring the signal. It consists of a series of pulses of $0.2 \mu\text{s}$ separated by a time of the order of T_2 forcing the nuclear spins to lose their coherence. A standard spin-echo sequence is applied after a while to detect the amplitude of the magnetization that has recovered equilibrium. Note that, unlike for T_2 measurements, no substantial frequency dependence of T_1 was observed, neither in pure EuO nor in Gd doped EuO.

Barak, Gabai and Kaplan determined that the spin-lattice relaxation in powdered EuO in an external magnetic field at temperatures below 14 K are dominated by two-magnon processes.⁴³ Also, between 14 K and 20 K, they observed that a three-magnon process surpasses the two-magnon process and that it is enhanced by a second-order three-magnon process. The results we obtained at

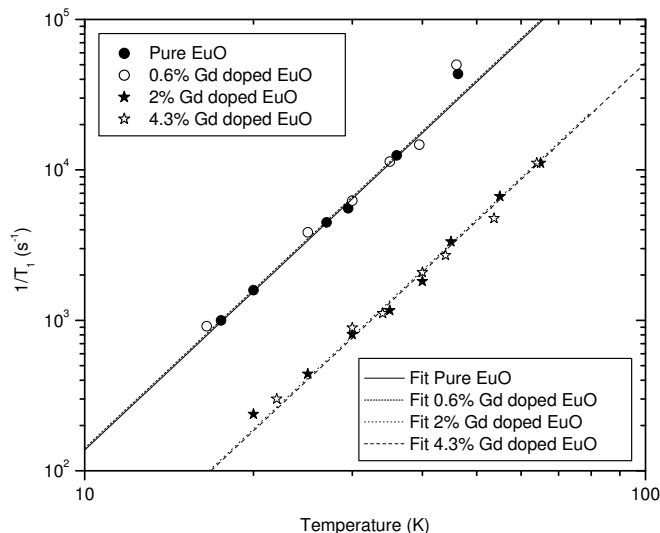


FIG. 5: Zero-field spin-lattice relaxation rates of ^{153}Eu in pure and Gd doped EuO as a function of temperature. The expression used to fit the curves is defined in (7).

zero-field confirmed that, for temperatures above about 14 K, the three-magnon process is the dominant spin-lattice relaxation process in EuO. The relaxation rate (Fig. 5) was found proportional to $T^{7/2}$. This is consistent with the temperature dependence of the theoretical expression first derived by Oguchi and Keffer for a three-magnon process.⁴⁴ We rederived the expression and adapted it to the case of zero-field measurements to obtain (Appendix A):

$$\frac{1}{T_1} = \frac{11.29}{16(2\pi)^5} \frac{A^2}{2JS \cdot \hbar S} \left(\frac{k_B T}{2JS} \right)^{7/2}, \quad (7)$$

where A is the hyperfine constant, $J = J_1 + J_2$ the exchange integral, S the electron spin, and k_B the Boltzmann constant. As for the results of Barak *et al.*, we had to multiply the expression (7) by the exchange scattering enhancement factor that we determined to be $\xi \cong 8$, in agreement with the calculation of Beeman and Pincus.⁴⁵ Taking $S = 7/2$ and determining A from the zero-field resonance frequency extrapolated to $T = 0$ K, $A = -\hbar\omega/S \cong -2.6 \cdot 10^{-26}$ J, we deduced from the fit a value of the exchange integral of $J/k_B = 0.755 \pm 0.01$ K.

NMR thus provides an accurate determination of J . Even if the enhancement factor is not precisely known, the fact that $1/T_1$, and therefore ξ/T_1 , is proportional to $J^{-9/2}$ (c.f. (7)) means that a large change in ξ leads to a small change in J . The influence of a variation in the enhancement factor on the determination of J is therefore limited, and we evaluated the error to be less than 1%. The other causes of uncertainty are the error on the T_1 measurement and the error on the temperature measurement. An evaluation of the total error leads to $\Delta J/k_B = 0.01$ K.

TABLE III: Values of J as a function of Gd doping.

Doping level x (%)	Exchange integral J/k_B (K)
0	0.755 ± 0.01
0.6	0.750 ± 0.01
2	1.205 ± 0.01
4.3	1.210 ± 0.01

Previous measurements on powdered EuO by neutron scattering experiments and specific heat measurements led respectively to $(J_1 + J_2)/k_B = 0.725 \pm 0.006$ K,⁴⁶ and $(J_1 + J_2)/k_B = 0.714 \pm 0.007$ K.⁴⁷ More recently, Mook measured single crystals of EuO by neutron scattering methods and he obtained the following values: $J_1/k_B = 0.625 \pm 0.007$ K and $J_2/k_B = 0.125 \pm 0.01$ K.⁴⁸ These values lead to a value of the exchange integral $J = 0.750 \pm 0.017$ K which is in very good agreement with our measurement. Note that in 1966 E. L. Boyd deduced J_1 and J_2 by measuring the temperature dependence of the NMR frequency of ^{153}Eu .³³ He found a value of $J_1/k_B = 0.750 \pm 0.0025$ K that is very close to the value of J that we determined. However, he deduced a negative value of J_2 .

In Gd doped EuO (Fig. 5), we observed that the temperature dependence of the spin-lattice relaxation times is the same $T^{7/2}$. Hence, as for pure EuO, the three-magnon process is the dominant relaxation process. Using expression (7) and the enhancement factor $\xi = 8$, we deduced the values of J shown in Table III for the doped samples. Clearly, the samples can be separated in two categories according to their value of J (Fig. 5).

To the best of our knowledge, no direct measurement of the exchange integral in Gd doped EuO has ever been published and our results provide therefore the first measurement of J in Gd doped EuO.

B. Spin-spin relaxation times

We performed spin-spin relaxation measurements in pure EuO and in Gd doped EuO using a standard spin-echo sequence composed of two consecutive pulses of duration t_1 and t_2 separated by a varying delay. Typical values were $t_1 = 0.1 \mu\text{s}$ and $t_2 = 0.2 \mu\text{s}$. Since T_2 is strongly frequency dependent, it is necessary to specify at what frequency it was measured. In the following, T_2 always corresponds to the spin-spin relaxation time measured at the frequency corresponding to the center of the central line, or the center of gravity of the line in case the central line is not well defined. Note that all the relaxation times that will be presented in the following correspond to measurements done with short delays. Therefore, the discussion and the analysis will focus on the fast decay times unless specified otherwise.

Except for the value of T_2 at 20.3 K determined by Uriano and Streever⁴² and the decay curve at 13.8 K published by Barak *et al.*,⁴⁹ there are no spin-spin re-

laxation time data for EuO above 4.2 K in the literature. However, several studies of T_2 at 4.2 K and lower temperatures were performed following the work of Barak *et al.*,^{49,50} Raj *et al.*,³⁴ Fekete *et al.*,⁵¹ the Lütgemeier group,^{28,29,39,52,53} and more recently Pieper *et al.*⁵⁴ The main reason for this interest is that the decay curve is not a single exponential. As Lütgemeier *et al.*²⁸ first noted, this is because there are two relaxation mechanisms: a fast one due to the Suhl-Nakamura indirect interaction, and a slow one due to direct dipolar coupling. However, the original Suhl-Nakamura theory fails to explain the observed spin-spin relaxation time and its frequency dependence that was first reported by Raj *et al.*³⁴ Barak *et al.* used the theory developed by Hone, Jaccarino, Ngwe and Pincus⁵⁵ (in the following we will refer to this theory as the HJNP theory) to explain why the value of T_2 they observed in a powdered EuO sample at 4.2 K is longer than the one predicted by the Suhl-Nakamura theory.⁴⁹ The HJNP theory assumes the existence of an inhomogeneous line broadening resulting from random microscopic inhomogeneities and predicts a frequency dependent T_2 . The HJNP theory predicts a Lorentzian line shape and for this reason we used a Lorentzian as magnetic distribution function in the calculation of the lineshape presented in Section II D.

In 1976, Fekete *et al.* successfully described the decay curves of the five transitions they had observed by assuming an inhomogeneous Suhl-Nakamura relaxation process (deduced from the HPJN model) and a dipolar coupling.⁵¹ They took into account all the elements necessary to describe the lineshape and its variation with delay as shown in Fig. 4. However, they did not discuss the implication of their results on the lineshape. Arons *et al.* published in 1975 the zero-field lineshape vs. delay and observed, as we did, the reduction of the amplitude of the central peak with increasing delay.²⁹ However, Arons *et al.* claimed that the T_2 of the central line was shorter because the signal was coming from nuclei located in domain walls. Our combined results on T_1 and T_2 measurements as a function of temperature point to more intrinsic mechanisms.

We measured the temperature dependence of the spin-spin relaxation times (Fig. 6). For pure EuO as well as for all the Gd doped samples, T_2 seems to be temperature independent at temperatures below about 15 K. For higher temperatures, we observed a rapid increase of the relaxation rates with increasing temperature. We analyze these two regimes below.

1. Lifetime effect

We saw in Sect. III A that the spin-lattice relaxation processes are dominated by the scattering of magnons by

nuclear spins, in particular by processes involving three magnons. One way to describe these processes is to consider the fluctuations of the hyperfine field. We can write

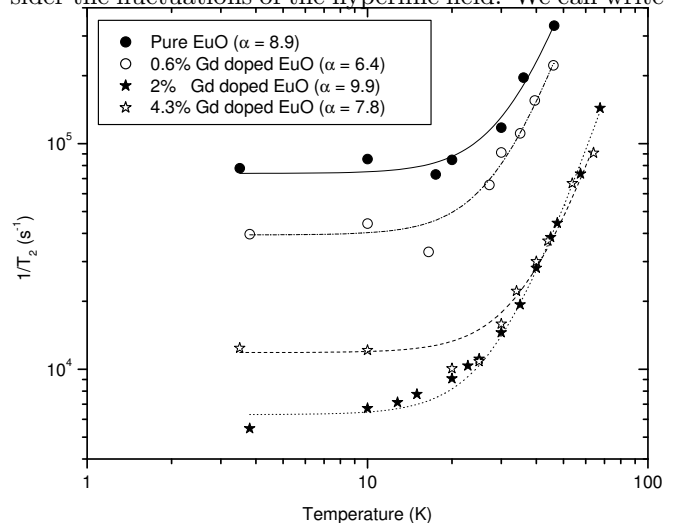


FIG. 6: Zero-field spin-spin relaxation rates of ^{153}Eu in pure and Gd doped EuO as a function of temperature. The parameter α and the fitting curve are defined in (9).

the perturbation Hamiltonian as

$$\hat{\mathcal{H}}_{h,f}^{pert}(t) = -\gamma_n \hbar [H_x(t)\hat{I}_x + H_y(t)\hat{I}_y + H_z(t)\hat{I}_z], \quad (8)$$

where $H_x(t)$, $H_y(t)$ and $H_z(t)$ are the fluctuating fields at the nuclear site due to fluctuations of $\hat{\mathbf{S}}$ in the x , y and z directions respectively.⁶⁵ The relaxation rates deriving from these interactions can be calculated using the Redfield theory.³⁷ The calculation for the particular case of a spin $I = \frac{5}{2}$ gives the following result for the spin-spin relaxation time:

$$\frac{1}{T_2} = \gamma_n^2 \overline{H_z^2} \tau_0 + \alpha \frac{1}{T_1}, \quad (9)$$

where $\overline{H_z^2}$ is the amplitude of the correlation function between $H_z(t)$ and $H_z(t + \Delta t)$, τ_0 is the correlation time (or lifetime) of the scattering process between the magnons and the nuclear spins, and

$$\alpha = I(I + 1) - m(m + 1) = \begin{cases} 5 & \text{for the } -5/2 \leftrightarrow -3/2 \text{ and } 3/2 \leftrightarrow 5/2 \text{ transitions} \\ 8 & \text{for the } -3/2 \leftrightarrow -1/2 \text{ and } 1/2 \leftrightarrow 3/2 \text{ transitions} \\ 9 & \text{for the } -1/2 \leftrightarrow 1/2 \text{ transition.} \end{cases} \quad (10)$$

We have assumed that the fluctuations of the three components of field x , y , and z are independent and that the correlation functions are simple exponential.³⁷ Since the length of the pulses as well as the amplitude of the RF field were chosen such as to excite all the transitions, we expect to have a mixture of these rates. As shown in Fig. 6, the factor α obtained from fitting the curves with the function $1/T_2 = \alpha/T_1 + \beta$ is between 6.3 and 9.9. This is in good agreement with the theoretical values (10). Therefore, according to the Redfield theory, the temperature dependence of the spin-spin relaxation in pure and Gd doped EuO is entirely determined by transverse fluctuating fields. Our results showed that these fluctuations were due to fluctuations of the electronic spins well described by spin-wave theory.

2. Temperature independent mechanisms

For temperatures far below the magnetic transition temperature, the Suhl-Nakamura interaction is expected to be temperature independent since its temperature dependence comes mostly from the hyperfine constant.^{56,57} The nuclear dipole-dipole interaction is also independent of temperature. Therefore, two processes compete and may be the source of the observed temperature independent T_2 's. In the case of pure EuO, the relaxation time due to the dipole-dipole interaction is considerably slower and we observed, in agreement with previous measurements, that the Suhl-Nakamura processes dominate the dipole-dipole processes for short delays. As shown in Fig. 6, the relaxation time of ^{153}Eu in Gd doped EuO is substantially slower than in pure EuO. In 2% Gd doped EuO at 3.8 K, we have measured $T_2 = 183 \mu\text{s}$. This value is very close to the value $T_2 = 194 \pm 2.4 \mu\text{s}$ deduced, following the treatment of Bohn *et al.*,⁵² from an exponential fit of the slow spin-echo decay measured in pure EuO and thought to be due to dipole-dipole interactions.⁶⁶

We observed that adding Gd in the EuO matrix leads to magnetic broadening, which increases with doping (c.f. Section IV). Therefore, in agreement with the HJNP theory, the replacement of Eu atoms by Gd atoms in the EuO matrix reduces the allowed mutual spin-flips between Eu nuclei leading to the Suhl-Nakamura relaxation and consequently we expect the relaxation rates to be smaller when the concentration of Gd is increased. The relaxation through dipole-dipole interactions is however still effective since in addition to the vanishing $\hat{I}_i^+ \hat{I}_j^-$ terms, the interaction Hamiltonian has diagonal $\hat{I}_{z,i} \hat{I}_{z,j}$ terms that do not vanish even if the frequencies of spins

i and j are very different. Note that the temperature independent relaxation rate is larger for 4.3% Gd doped EuO than for 2% Gd doped EuO. The presence of an increasing number of conduction electrons when the Gd concentration is increased above about 1.5% might introduce an additional relaxation process through an RKKY indirect interaction.

IV. MAGNETIC INHOMOGENEITIES

A. Temperature dependence of the pure EuO lineshape

To the best of our knowledge, no measurement of the lineshape of pure EuO above 4.2 K has ever been published. We report here the first study of the temperature dependence of the ^{153}Eu lineshape. In Fig. 7, we present the lineshape of pure EuO at 4.2 K and at several temperatures between 4.2 K and 42 K. These lines were obtained by Fourier transforming the spin-echo measured at the frequency of the center of the lines. Since, as shown in Section II C, the NMR frequency varies considerably with the temperature, we shifted the center of the lines presented in the figure to zero frequency in order to compare the lines recorded at different temperatures. We also adjusted the amplitude of the lines to superimpose the wings of all the lines. This adjustment allowed us to compare the amplitude and the width of the central peak of the lines.

We observed that the intensity of the central peak was greatly reduced with increasing temperature. As noted in Section III B, the spin-spin relaxation times are frequency dependent and they are shorter for frequencies close to the central peak. Also, we observed that T_2 is strongly temperature dependent, decreasing with increasing temperature. Therefore, we concluded that the intensity of the central peak decreased with increasing temperature as a consequence of the decreasing value of T_2 , our spectrometer not being able to detect all the nuclei of the central peak. We also observed that the width of the central peak increases almost linearly from about 0.11 MHz at 4.2 K to about 0.23 MHz at 41.4 K. This broadening mechanism did not seem to be linked to T_2 effects since we measured $T_2 \cong 4 \mu\text{s}$ at 41.4 K, which corresponds to a Lorentzian width of about 0.08 MHz.

Finally, we observed that the electrical quadrupole splitting decreases with increasing temperature. We estimated the change to be of the order of 25%, from $\Delta\nu_Q \cong 0.75 \text{ MHz}$ at 4.2 K to $\Delta\nu_Q \cong 0.55 \text{ MHz}$ at 41.4 K.

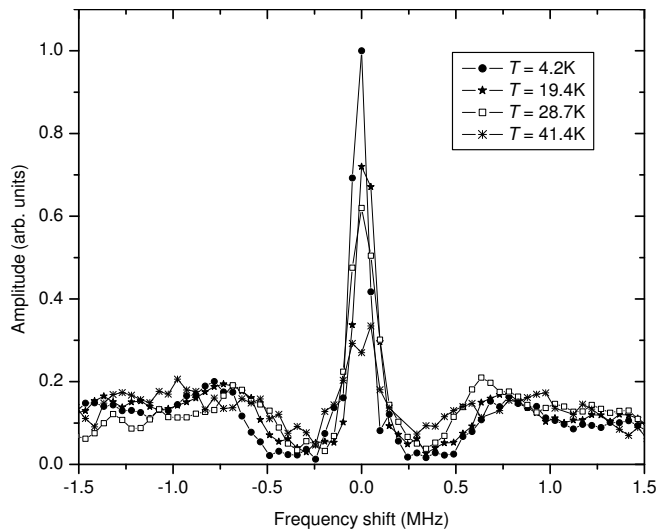


FIG. 7: Zero-field lineshape of ^{153}Eu in EuO vs. temperature. The lineshapes were obtained by Fourier transform of the spin-echo signal.

We think that this change might be due to a variation of the magnetostriction with temperature. This assumption is supported by the results of F. Levy who observed, by X-ray measurements, that the spontaneous magnetostriction of EuO decreases by about 25% between 4.2 K and 40 K.⁵⁸ Note that if the quadrupolar splitting was due to the presence of defects in the crystals, as was proposed by Arons *et al.*,³⁹ we would probably not observe such a temperature dependence.

B. Influence of Gd on EuO lineshape

We now turn to the analysis of the lineshapes of ^{153}Eu in Gd doped EuO. We observed that the frequency of the central transition of the 0.6% Gd doped EuO lineshape at 4.2 K was only slightly shifted towards higher frequency compared to pure EuO, from 138.45 MHz to 138.48 MHz. However, the central line was substantially broader as can be seen on Fig. 8. As discussed in Section IID, the width of the central transition is determined by magnetic broadening only. We think that the observed line at 4.2 K is broader in the 0.6% sample than in the pure sample because of the random distribution of Gd atoms in the EuO matrix. Since different Eu atoms have different numbers of nearest and next nearest Gd neighbors, the local field acting on Eu atoms, which is influenced by the presence of Gd, is not the same at each Eu site. Another noticeable difference between pure EuO and 0.6% Gd doped EuO is that the quadrupolar structure is not resolvable in 0.6% Gd doped EuO. We think that this is also due to the random distribution of Gd atoms in EuO which leads to a random distribution of EFGs.

We also measured the lineshape of 0.6% Gd doped EuO as a function of temperature from 4.2 K to 49.5 K (Fig. 8).

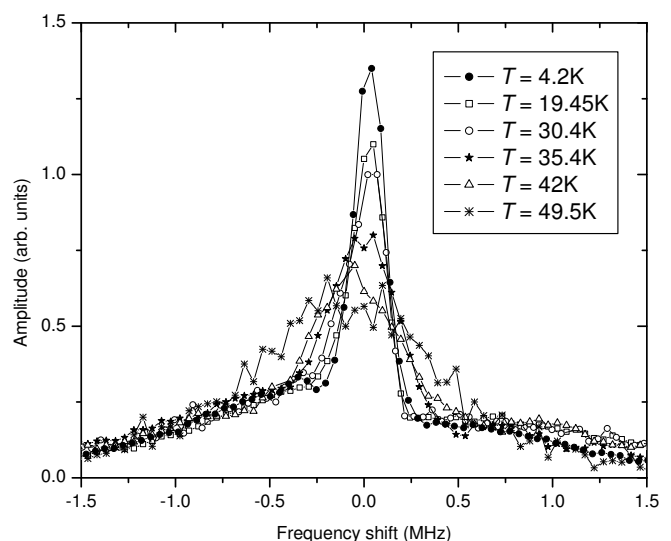


FIG. 8: Zero-field lineshape of ^{153}Eu in 0.6% Gd doped EuO vs. temperature. The lineshapes were obtained by Fourier transform of the spin-echo signal.

We observed a temperature dependent broadening of the central line. We adjusted the amplitude of the different lines by superimposing the wings of all the lines.⁶⁷ We plotted in Fig. 10 the full width at half maximum (FWHM) of the central line as a function of temperature for all the samples.⁶⁸ It appears that for temperatures above about 30 K, the FWHM of the 0.6% Gd doped EuO lineshape increases sharply with increasing temperature. We did not observe this phenomena in pure EuO. We demonstrate that the broadening could not be explained by a variation in T_2 and that the broadening was therefore a static broadening. Indeed, the measured $1/T_2$ is much less than the observed linewidth. Moreover, we observed that T_2 has the same temperature dependence in 0.6% Gd doped EuO as in pure EuO (c.f. Section III B), and the spin-spin relaxation rates in 0.6% Gd doped EuO are longer than in pure EuO.

The addition of 0.6% Gd in the EuO matrix gives rise to temperature dependent phenomena associated with a static magnetic inhomogeneity. The temperature dependent broadening mechanism initiates at about 30 K, the temperature at which the conductivity starts decreasing dramatically according to the results of Godart *et al.*¹⁵ and Samokhvalov *et al.*¹⁴ This suggests that the phenomena we observed at the level of the hyperfine field are likely to be related to the transport properties of the material and in particular to CMR.

Magnetic entities such as magnetic polarons are thought to play a crucial role in these materials. In particular, they are thought to be the main cause of CMR. We will show below that a simple model assuming that magnetic entities are present in the material and give rise to the static NMR line broadening, which we observe at higher temperatures, is not consistent with the observed relaxation times.

Suppose that in order to explain the narrow lines at low temperatures, we assume the magnetic entities diffuse rapidly at low temperatures, giving rise to motional narrowing. Thus they would create a fluctuating field at the nuclear site with correlation time τ . The relaxation time deriving from the presence of this fluctuating field could then be written

$$\frac{1}{T_2} = \frac{\delta\omega^2\tau}{1 + (\delta\omega\tau)^2} \quad (11)$$

where $\delta\omega$ is the distribution in NMR frequency caused by the fluctuating magnetic field.³⁷ Since we observed that the line is broadened at high temperature, we assume that at high temperature the correlation time is long, i.e. $T_2 \cong \tau$. This is consistent with the model of magnetic polarons, since magnetic polarons are thought to be trapped at high temperature (leading to a decrease in conductivity). At low temperature we assume that the entities are moving, which means that τ is short. In this case, $1/T_2 \cong \delta\omega^2\tau$ and the line is motional narrowed. In between the high temperature regime and the low temperature regime, we expect that $\delta\omega\tau = 1$ at a given temperature. At that temperature, $1/T_2$ is maximum and $T_2 = 2\tau = 2/\delta\omega$. Assuming that $\delta\omega$ is temperature independent, that means that the relaxation rate is about equal to the static linewidth at high temperatures. But in fact, at all temperatures $1/T_2$ is much less than the observed line width. Thus we cannot explain the data consistently with this model. Instead, we can argue from NMR that the material at low temperatures is spatially uniform, but as the temperature rises, non-uniformities set in.

We also measured the effect of an external magnetic field of 4T on the temperature dependence of the FWHM of the line. A field of 4T was strong enough to saturate the magnetization, and as a consequence a non-negligible demagnetizing field was present in the non-perfectly ellipsoidal sample. Because of the inhomogeneity in the demagnetizing field, we measured a FWHM of about 0.5 MHz at 10K, which was about 2.5 times broader than the zero-field FWHM at the same temperature. However, the FWHM did not increase with increasing temperature, and it was still about 0.5 MHz at 50 K. We concluded that the temperature dependent static inhomogeneities that we measured at zero-field were not present when there was a strong external magnetic field. This observation is an additional suggestion that the broadening might be linked to transport properties of the material. Indeed, since the conductivity of CMR materials is increased by the application of an external magnetic field, applying a field might perhaps be viewed as equivalent to lowering the temperature, as far as the transport properties are concerned.¹¹ Therefore, at a given temperature we can expect the line to be narrower in the presence of an external field than in zero-field.

The center of the 2% and 4.3% Gd doped EuO lines are considerably shifted towards higher frequency

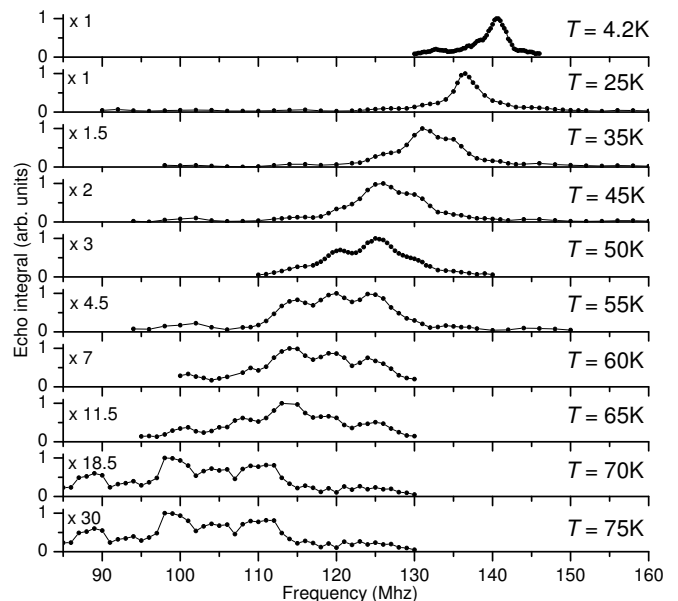


FIG. 9: Zero-field lineshape of Eu^{153} in 2% Gd doped EuO vs. temperature. The amplitude of the lineshape was multiplied by the coefficient shown on the left side of each curve.

(140.6 MHz and 140.0 MHz respectively). However, we did not observe a monotonic increase of the shift with the doping, the shift being smaller for 4.3% Gd doped EuO than for 2% Gd doped EuO. We also observed that increasing the Gd doping strongly influences the shape of the ^{153}Eu line (c.f. Fig. 9). In particular, the lines of 2% and 4.3% Gd doped samples were considerably broader than in the case of pure EuO and 0.6% Gd doped EuO and we could not distinguish the central transition from the other transitions. In order to decide whether or not this broadening mechanism was magnetic in origin, we measured the ^{151}Eu lineshape of the 4.3% sample and we compare the ^{153}Eu and ^{151}Eu lineshapes. The frequency of the ^{151}Eu lineshape was multiplied by the ratio $^{151}\gamma_n/^{153}\gamma_n$. Since the two curves had a similar shape, we concluded that the broadening mechanism was of magnetic origin. We do not know exactly what interaction causes this large broadening, but we do know from the T_2 measurements (c.f. Sect. III B) that the broadening is a static broadening. In conclusion, we observed a remarkable difference between the lineshape of samples with none or low Gd doping and the lineshape of samples with higher Gd doping.

We also measured the temperature dependence of the ^{153}Eu lineshape in 2% and 4.3% Gd doped EuO. We plotted the measurements for 2% Gd doped EuO in Fig. 9. A similar temperature behavior was observed in 4.3% Gd doped EuO. We performed point-by-point measurements to determine the lineshapes. Note that at temperatures higher than about 80 K we could not detect the resonance. This failure was probably due to the fact that the line was too broad and therefore the signal was too weak.

As shown in Fig. 9, the lineshape becomes broader with

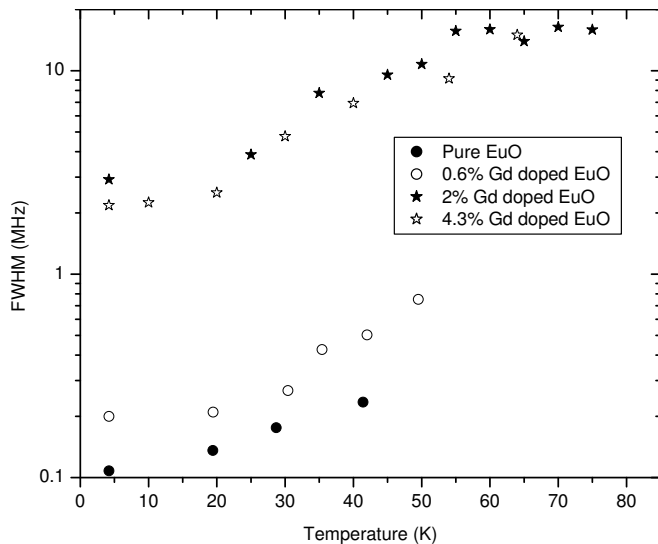


FIG. 10: FWHM of the zero-field lineshape of Eu^{153} in pure EuO and 0.6%, 2% and 4.3% Gd doped EuO vs. temperature.

increasing temperature. Also, the structure of the lineshape becomes more and more complex with increasing temperature. In Fig.10 we plotted the FWHM of the lineshape as a function of temperature for 2% and 4.3% Gd doped EuO along with the temperature dependence of the FWHM of the lineshape of pure EuO and 0.6% Gd doped EuO. At temperatures above about 50 K the FWHM of 2% and 4.3% Gd doped EuO is ill-defined since the line has a complex shape. We determined that the temperature dependent broadening was magnetic in origin and since $1/T_2$ is by far smaller than the linewidth of the lines we measured, we concluded that the temperature dependent broadening is a static magnetic broadening.

A possible explanation for the temperature dependent broadening in 2% and 4.3% Gd doped EuO is that the value of the exchange integral is distributed throughout the samples, i.e., different part of the samples have different values of J . For any reasonable model of $M(T)$, it would take a large change in T_C , hence of J , to account for the spread in frequency we observed. However, a slight variation of J strongly influences the value of T_1 because $T_1 \propto J^{9/2}$. We observed that the measured T_1 was, to a good approximation, independent of the position on the line. Therefore, we must conclude that there is a negligible distribution in J .

V. CONCLUSIONS

The study of pure and Gd doped EuO was motivated by the unconventional electrical and magnetic properties observed in this system. Our NMR measurements led to results giving new information on the microscopic magnetic properties of Gd doped EuO. We observed a dramatic difference between pure or nearly pure (0.6%

Gd doped) samples, and samples with higher Gd concentration both in static and dynamic magnetic properties. Below are the main outcomes of this study.

1. Exchange integral J vs. doping

We observed that the relaxation times in pure and Gd doped EuO were in good agreement with a law derived from spin-wave theory for temperatures as high as $T \cong 0.6 T_C$. From the temperature dependence of the relaxation times, we inferred the value of the exchange integral J as a function of Gd doping. We observed an abrupt increase of the amplitude of the exchange interaction with doping. This is consistent with the dependence on Gd concentration of the Curie temperature for which different theoretical explanations have been proposed by Mauger *et al.*,^{31,59} Nolting and Oleś,⁶⁰ and more recently Santos and Nolting.⁹

2. Variation of static magnetic broadening with temperature in Gd doped EuO

We discovered that the lineshape of the Eu resonance in Gd doped EuO was broader than in pure EuO and that the broadening increases abruptly with Gd concentration. We also observed that the broadening increases with increasing temperature. We showed that the broadening was due to inhomogeneities in the local magnetic field acting on the Eu nuclei. We confirmed that the increase in broadening was not due to temperature dependent fluctuations of the electron spins. $1/T_2$ was shown to be determined by these fluctuations, but was considerably smaller than the width of the broadening. Thus, the magnetic inhomogeneities were static at all temperatures, at least at the time scale of NMR, which is of the order of several microseconds. Cooper *et al.*, who studied Gd doped EuO by Raman spectroscopy, also observed magnetic inhomogeneities in Gd doped EuO.^{2,4,61} Our results confirm theirs but we can go further by affirming that the inhomogeneities are static.

In 0.6% Gd doped EuO, we observed that above about 30 K the magnetic inhomogeneity increases rapidly with increasing temperature. According to previous transport measurements, the resistivity of samples containing a similar Gd concentration increases dramatically above about 30 K.^{14,15} This suggests that the broadening mechanism is linked to the change in transport properties of the sample. Numerous models explain this change in transport properties by the formation of bound magnetic polarons. We could rule out the picture according to which the localized magnetic entities were highly mobile at low temperatures, giving motionally narrowed lines and high conductivity.

In samples with higher Gd concentration (2% and 4.3%), the observed static broadening is much larger than in 0.6% Gd doped EuO. Also, above about 30 K, some

structure develops in the lineshape along with the increase of magnetic inhomogeneity in the samples. We showed that this phenomenon was not due to a distribution in the value of the exchange integral J .

We must conclude that at low temperatures the magnetic phase of the Gd doped samples is fairly homogeneous, and that static magnetic inhomogeneities are formed when the temperature is increased. From our results, we deduce that a theory to be valid has to include a spatially homogeneous and temperature independent J , but include the presence of magnetic inhomogeneities. Therefore, the explanation of the magnetization curve given by Borukhovich *et al.* is incompatible with our results since it assumes a distribution of J in the sample.⁶² Although both the theories of Mauger *et al.*³¹ and Noltling *et al.*⁶⁰ assume a spatially homogeneous J and seem to correctly describe the doping dependence of the Curie temperature, they both suppose that J is temperature dependent, which in the light of our results cannot be the case. In addition, these models assume that the magnetization is uniform within the sample, i.e. they do not take into account any magnetic inhomogeneities.

There remains the possibility that the charge carrier trapping above about 30 K that accounts for the dramatic temperature dependence of the electrical resistivity causes a distribution in hyperfine field, presumably because the charge carriers are not all in the same spin state. This description is compatible with a theory based

on the formation of magnetic polarons taken to be static on the NMR time scale. However, to the best of our knowledge, a complete model containing all the key features of the Gd doped EuO systems does not yet exist.

Acknowledgments

We are very grateful to Dylan F. Smith for his invaluable help during the various experiments. We also would like to thank K. Mattenberger for providing the samples. This work was supported by the U.S. Department of Energy, Division of Materials Sciences, through the Frederick Seitz Materials Research Laboratory at the University of Illinois at Urbana-Champaign under Award No. DEFG02-91ER45439.

APPENDIX A: THREE-MAGNON RELAXATION PROCESS

Below we present the derivation of the formula giving the relaxation rate due to three-magnon relaxation process for the case of zero-field NMR in a ferromagnet with low anisotropy. Using a similar derivation than the one leading to (14) in the paper of Barak *et al.*,⁴³ we obtained:

$$\begin{aligned} \frac{1}{T_1} &= \frac{\pi A^2 a^9}{8\hbar S} \int_0^\infty \int_0^\infty \frac{\exp((\epsilon_{\mathbf{k}_1} + g\mu_B|\mathbf{H}|)/k_B T)}{\exp((\epsilon_{\mathbf{k}_1} + g\mu_B|\mathbf{H}|)/k_B T) - 1} \\ &\times \frac{\exp((\epsilon_{\mathbf{k}_2} + g\mu_B|\mathbf{H}|)/k_B T)}{\exp((\epsilon_{\mathbf{k}_2}/k_B T + g\mu_B|\mathbf{H}|)) - 1} \frac{g(\epsilon_{\mathbf{k}_1})g(\epsilon_{\mathbf{k}_1})g(\epsilon_{\mathbf{k}_2} + \epsilon_{\mathbf{k}_2})d\epsilon_{\mathbf{k}_1}d\epsilon_{\mathbf{k}_2}}{\exp((\epsilon_{\mathbf{k}_1} + \epsilon_{\mathbf{k}_2} + 2g\mu_B|\mathbf{H}|)/k_B T) - 1}. \end{aligned} \quad (\text{A1})$$

where a is the lattice constant of the crystal (we used the fact that EuO and Gd doped EuO are cubic crystals), g is the g-factor, μ_B is the Bohr magneton, $\mathbf{H} = \mathbf{H}_{an} + \mathbf{H}_0 + \mathbf{H}_{dm}$, where \mathbf{H}_{an} is the anisotropy field, \mathbf{H}_0 is the applied external field, and \mathbf{H}_{dm} is the demagnetization field, $\epsilon_{\mathbf{k}_i}$ is the spin-wave energy, and $g(\epsilon_{\mathbf{k}_i})$ is the density

of states of the spin waves. We then used the fact that the low energy spin waves give the principal part of the integral in (A1),⁴³ and we therefore determined $g(\epsilon_{\mathbf{k}_i})$ by using the approximation $\epsilon_{\mathbf{k}_i} = 2JS\mathbf{k}_i^2 a^2$. We obtained:

$$\begin{aligned} \frac{1}{T_1} &= \frac{1}{16(2\pi)^5} \frac{A^2}{2JS \cdot \hbar S} \frac{1}{(2JS)^{7/2}} \int_0^\infty \int_0^\infty \frac{\exp((\epsilon_{\mathbf{k}_1} + g\mu_B|\mathbf{H}|)/k_B T)}{\exp((\epsilon_{\mathbf{k}_1} + g\mu_B|\mathbf{H}|)/k_B T) - 1} \\ &\times \frac{\exp((\epsilon_{\mathbf{k}_2} + g\mu_B|\mathbf{H}|)/k_B T)}{\exp((\epsilon_{\mathbf{k}_2}/k_B T + g\mu_B|\mathbf{H}|)) - 1} \frac{\sqrt{\epsilon_{\mathbf{k}_1}^2 \epsilon_{\mathbf{k}_2} + \epsilon_{\mathbf{k}_2}^2 \epsilon_{\mathbf{k}_1}}}{\exp((\epsilon_{\mathbf{k}_1} + \epsilon_{\mathbf{k}_2} + 2g\mu_B|\mathbf{H}|)/k_B T) - 1} d\epsilon_{\mathbf{k}_1} d\epsilon_{\mathbf{k}_2}. \end{aligned} \quad (\text{A2})$$

Beeman and Pincus used the fact that $k_B T \gg g\mu_B|\mathbf{H}|$, and they found the integral in (A2) to be equal to

$7.6(k_B T)^{7/2}$ (c.f. (2.22) in the article of Beeman and

Pincus⁶⁹).⁴⁵ We recomputed the integral in order to obtain a value adapted to the case of zero-field NMR measurements of Eu nuclei in EuO and Gd doped EuO. In that case, $|\mathbf{H}| = |\mathbf{H}_{an}|$ and at 4.2 K the ratio $g\mu_B|\mathbf{H}_{an}|/k_B T$ is approximately equal to $8 \cdot 10^{-3}$. Since we observed that the three-magnon process is the main relaxation process for temperatures between about 15 K and 50 K, we had to take a substantially smaller value of $g\mu_B|\mathbf{H}|/k_B T$. Taking $T = 30$ K and $|\mathbf{H}_{an}(T = 30 \text{ K})|/|\mathbf{H}_{an}(T = 4.2 \text{ K})| \cong 2.5$,²⁵ we obtained $g\mu_B|\mathbf{H}|/k_B T \cong 4 \cdot 10^{-4}$. With this value, we evaluated the integral to be approximately $10.5 (k_B T)^{7/2}$. This value is very close to the value obtained if we as-

sume $g\mu_B|\mathbf{H}|/k_B T = 0$, and since there is no apparent reason to compute the integral with $T = 30$ K instead of any other temperature in the range $15 \text{ K} < T < 50 \text{ K}$, we decided to use the result corresponding to the approximation $g\mu_B|\mathbf{H}|/k_B T = 0$, that is $11.29 (k_B T)^{7/2}$. This result leads to the expression given in (7).

Since we were interested in evaluating J using (A2), we had to determine the influence of a variation in the value of the integral on J . We calculated that if the factor 11.29 is replaced by the factor 10.5 obtained for $T = 30$ K, the value of J would be changed by about 1%. Therefore we decided that (7) could be used to determine a fairly accurate value of J from our data.

* Electronic address: arnaud.comment@epfl.ch

† Present address: Department of Physics, Chonbuk National University, Jeonju 561-756, Korea.

- ¹ B. T. Matthias, R. M. Bozorth, and J. H. Van Vleck, *Phys. Rev. Lett.* **7**, 160 (1961).
- ² C. S. Snow, S. L. Cooper, D. P. Young, Z. Fisk, A. Comment, and J.-P. Ansermet, *Phys. Rev. B* **64**, 174412 (2001).
- ³ P. G. Steeneken, L. H. Tjeng, I. Elfimov, G. A. Sawatzky, G. Ghiringhelli, N. B. Brookes, and D.-J. Huang, *Phys. Rev. Lett.* **88**, 047201 (2002).
- ⁴ H. Rho, C. S. Snow, S. L. Cooper, Z. Fisk, A. Comment, and J.-P. Ansermet, *Phys. Rev. Lett.* **88**, 127401 (2002).
- ⁵ J. Lettieri, V. Vaithyanathan, S. K. Eah, J. Stephens, V. Sih, D. D. Awschalom, J. Levy, and D. G. Schlom, *Appl. Phys. Lett.* **83**, 975 (2003).
- ⁶ H. Ohno, *Science* **281**, 951 (1998).
- ⁷ P. Ball, *Nature* **404**, 918 (2000).
- ⁸ R. Schiller and W. Nolting, *Phys. Rev. Lett.* **86**, 3847 (2001).
- ⁹ C. Santos and W. Nolting, *Phys. Rev. B* **65**, 144419 (2002).
- ¹⁰ P. Sinjukow and W. Nolting, *Phys. Rev. B* **68**, 125107 (2003).
- ¹¹ Y. Shapira, S. Foner, and T. B. Reed, *Phys. Rev. B* **8**, 2299 (1973).
- ¹² M. R. Oliver, J. A. Kafalas, J. O. Dimmock, and T. B. Reed, *Phys. Rev. Lett.* **24**, 1064 (1970).
- ¹³ G. Petrich, S. von Molnár, and T. Penney, *Phys. Rev. Lett.* **26**, 885 (1971).
- ¹⁴ A. A. Samokhvalov, N. A. Viglin, B. A. Gizhevskii, T. I. Arbutova, and N. M. Chebotaev, *Phys. Status Solidi B* **148**, 361 (1988).
- ¹⁵ C. Godart, A. Mauger, J. P. Desfours, and J. C. Achard, *J. Phys.* **41**, C5, 205 (1980).
- ¹⁶ G. Papavassiliou, M. Fardis, M. Belesi, T. G. Maris, G. Kallias, M. Pissas, D. Niarchos, C. Dimitropoulos, and J. Dolinsek, *Phys. Rev. Lett.* **84**, 761 (2000).
- ¹⁷ G. Papavassiliou, M. Pissas, M. Belesi, M. Fardis, J. Dolinsek, C. Dimitropoulos, and J.-P. Ansermet, *Phys. Rev. Lett.* **91**, 147205 (2003).
- ¹⁸ J. Schoenes and P. Wachter, *Phys. Rev. B* **9**, 3097 (1974).
- ¹⁹ A. Comment and J.-P. Ansermet (to be published in *J. Magn. Reson.*).
- ²⁰ E. A. Turov and M. P. Petrov, *Nuclear Magnetic Resonance in Ferro- and Antiferromagnets* (John Wiley & Sons, New York, 1972).
- ²¹ A. C. Gossard and A. M. Portis, *Phys. Rev. Lett.* **3**, 164 (1959).
- ²² A. M. Portis and A. C. Gossard, *J. Appl. Phys.* **31**, 205S (1960).
- ²³ A. Flossdorff, D. Görlitz, and J. Köstler, *J. Appl. Phys.* **79**, 6054 (1996).
- ²⁴ A. A. Samokhvalov, V. G. Bamburov, N. V. Volkenshteyn, T. D. Zotov, A. Ivakin, Y. N. Morozov, and M. I. Simonova, *Fiz. Metal. i Metalloved* **20**, 308 (1964).
- ²⁵ R. S. Hughes, G. E. Everett, and A. W. Lawson, *Phys. Rev. B* **9**, 2394 (1974).
- ²⁶ A. Kasuya and M. Tachiki, *Phys. Rev. B* **8**, 5298 (1973).
- ²⁷ D. Fekete, N. Kaplan, and T. B. Reed, *Solid State Comm.* **15**, 1827 (1974).
- ²⁸ H. Luetgemeier, R. R. Arons, and H. G. Bohn, *Proceedings of XVIIIth Ampere Congress* (Nottingham, 1974).
- ²⁹ R. R. Arons, H. G. Bohn, and H. Luetgemeier, *Physica B* **80**, 12 (1975).
- ³⁰ A. A. Samokhvalov, T. I. Arbutova, M. I. Simonova, and L. D. Fal'kovskaya, *Fizika Tv. Tela* **15**, 3690 (1973).
- ³¹ A. Mauger, C. Godart, M. Escorne, J. C. Achard, and J. P. Desfours, *J. Phys.* **39**, 1125 (1978).
- ³² C. Kapusta, P. C. Riedi, W. Kocemba, G. J. Tomka, M. R. Ibarra, J. M. D. Teresa, M. Viret, and J. M. D. Coey, *J. Phys.: Condens. Matter* **11**, 4079 (1999).
- ³³ E. L. Boyd, *Phys. Rev.* **145**, 174 (1966).
- ³⁴ K. Raj, T. J. Burch, and J. I. Budnick, *Int. J. Magnetism* **3**, 355 (1972).
- ³⁵ H. G. Bohn, R. R. Arons, and H. Luetgemeier, *Proceedings of XVIIIth Ampere Congress* (Nottingham, 1974).
- ³⁶ *CRC Handbook of Chemistry and Physics* (CRC Press, 2003), 84th ed.
- ³⁷ C. P. Slichter, *Principles of Magnetic Resonance* (Springer-Verlag, 1990), 3rd ed.
- ³⁸ W. J. Thompson, *Computers in Physics* **7**, 627 (1993).
- ³⁹ R. R. Arons, H. G. Bohn, K. J. Fischer, and H. Luetgemeier, *Solid State Comm.* **26**, 625 (1978).
- ⁴⁰ E. L. Boyd, *Bull. Am. Phys. Soc.* **8**, 439 (1963).
- ⁴¹ S. H. Charap and E. L. Boyd, *Phys. Rev.* **133**, A811 (1964).
- ⁴² G. A. Urriano and R. L. Streever, *Phys. Lett.* **17**, 205 (1965).
- ⁴³ J. Barak, A. Gabai, and N. Kaplan, *Phys. Rev. B* **9**, 4914 (1974).
- ⁴⁴ T. Oguchi and F. Keffer, *J. Phys. Chem. Solids* **25**, 405 (1964).

- ⁴⁵ D. Beeman and P. Pincus, Phys. Rev. **166**, 359 (1968).
- ⁴⁶ L. Passell, O. W. Dietrich, and J. Als-Nielsen, Phys. Rev. B **14**, 4897 (1976).
- ⁴⁷ O. W. Dietrich, J. A. J. Henderson, and H. Meyer, Phys. Rev. B **12**, 2844 (1975).
- ⁴⁸ H. A. Mook, Phys. Rev. Lett. **46**, 508 (1981).
- ⁴⁹ J. Barak, I. Siegelstein, A. Gabai, and N. Kaplan, Phys. Rev. B **8**, 5282 (1973).
- ⁵⁰ J. Barak, I. Siegelstein, A. Gabai, and N. Kaplan, Phys. Rev. Lett. **27**, 817 (1971).
- ⁵¹ D. Fekete, N. Kaplan, and T. B. Reed, Phys. Lett. **55A**, 356 (1976).
- ⁵² H. G. Bohn, R. R. Arons, H. Luetgemeier, and K. J. Fischer, J. Mag Mag. Mat. **2**, 67 (1976).
- ⁵³ R. R. Arons, H. G. Bohn, and H. Luetgemeier, Physica B **86-88**, 1303 (1977).
- ⁵⁴ M. W. Pieper, D. Baetjer, and K. Fischer, Z. Phys. B **98**, 1 (1995).
- ⁵⁵ D. Hone, V. Jaccarino, T. Ngwe, and P. Pincus, Phys. Rev. **186**, 291 (1969).
- ⁵⁶ H. Suhl, Phys. Rev. **109**, 606 (1958).
- ⁵⁷ T. Nakamura, Progr. Theor. Phys. **20**, 542 (1958).
- ⁵⁸ F. Levy, Phys. Kond. Mater. **10**, 71 (1969).
- ⁵⁹ A. Mauger, Phys. Status Solidi B **84**, 761 (1977).
- ⁶⁰ W. Nolting and A. M. Oleś, Z. Phys. B **43**, 37 (1981).
- ⁶¹ H. Rho, C. S. Snow, S. L. Cooper, Z. Fisk, A. Comment, and J.-P. Ansermet, Physica B **312-313**, 775 (2002).
- ⁶² A. S. Borukhovich, V. G. Bamburov, and A. A. Sidorov, J. Mag Mag. Mat. **73**, 106 (1988).
- ⁶³ Since the central peak is sharp, the echo is long and it was not possible to use delays shorter than about 10 μ s to record the entire echo, even with the short recovery time of 0.3 μ s of the receiver.
- ⁶⁴ From the above analysis, we deduced a ratio $^{151}\gamma_n/^{153}\gamma_n$ slightly different than the one given in tables. Indeed, by comparing the frequency of the central transition of both isotopes, we obtained a ratio of about 2.254 and the value given in tables is about 2.2645.³⁶
- ⁶⁵ We do not need to make any assumption on the anisotropy of the hyperfine coupling. This expression is valid even if the hyperfine coupling needs to be describe by a tensor.
- ⁶⁶ The dipole-dipole relaxation time in Gd doped EuO is expected to be slightly longer than in pure EuO due to the fact that interactions between Eu nuclear spins and Gd nuclear spins (unlike spins) lead to less effective relaxation processes.³⁷
- ⁶⁷ While the intensity of the central line in pure EuO was decreasing with increasing temperature due to short T_2 's, we observed that the area under the central peak of 0.6% Gd doped EuO was to a good approximation temperature independent. This is most likely because the spin-spin relaxation times in 0.6% Gd doped EuO are slower by a factor of about 1.5.
- ⁶⁸ We defined the half maximum of the central line of 0.6% Gd doped EuO from the top of the wings and not from zero intensity. Therefore, we probably underestimated the FWHM of the lineshape of 0.6% Gd doped EuO.
- ⁶⁹ There is an error in equation (2.22) where $h^{7/2}$ should be replaced by $\hbar^{7/2}$.